J Stat Phys manuscript No.
(will be inserted by the editor)

Eigenvector localization in real networks and its implications for epidemic spreading

Romualdo Pastor-Satorras · **Claudio Castellano**

arXiv:1801.05649v1 [physics.soc-ph] 17 Jan 2018

Received: date / Accepted: date

Abstract The spectral properties of the adjacency matrix, in particular its largest eigenvalue and the associated principal eigenvector, dominate many structural and dynamical properties of complex networks. Here we focus on the localization properties of the principal eigenvector in real networks. We show that in most cases it is either localized on the star defined by the node with largest degree (hub) and its nearest neighbors, or on the densely connected subgraph defined by the maximum K-core in a K-core decomposition. The localization of the principal eigenvector is often strongly correlated with the value of the largest eigenvalue, which is given by the local eigenvalue of the corresponding localization subgraph, but different scenarios sometimes occur. We additionally show that simple targeted immunization strategies for epidemic spreading are extremely sensitive to the actual localization set.

Keywords Complex networks · Spectral properties · Dynamical processes

1 Introduction

The adjacency matrix encodes all the information about a complex network [21] and, as a consequence, about its structure and function. The knowledge of its spectral properties provides a fundamental tool to understand the network topology and the behavior of dynamical processes mediated by it [1]. In particular the largest eigenvalue (LEV) Λ_M of the adjacency matrix determines the position of critical transitions for processes as diverse as epidemics [7,3,12], synchronization [26], weighted percolation on directed networks [28], models of genetic control [25], or the dynamics of excitable elements [17]. On the other hand, the principal eigenvector (PEV), $\{f_i\}$, corresponding to the LEV, is at the core of a

We acknowledge financial support from the Spanish MINECO, under Projects No. FIS2013-47282-C2-2 and No. FIS2016-76830-C2-1-P. R. P.-S. acknowledges additional financial support from ICREA Academia, funded by the Generalitat de Catalunya.

Romualdo Pastor-Satorras
Departament de Física i Enginyeria Nuclear, Universitat Politècnica de Catalunya, Campus Nord B4, 08034 Barcelona, Spain

Claudio Castellano
Istituto dei Sistemi Complessi (ISC-CNR), via dei Taurini 19, I-00185 Roma, Italy
Dipartimento di Fisica, "Sapienza" Università di Roma, P.le A. Moro 2, I-00185 Roma, Italy

set of centrality measures, such as Katz's centrality [16] or PageRank [2], and it has been associated with the validity of mean-field approaches for the study of epidemic spreading in networks [12].

A fundamental problem in network science is hence the understanding of how Λ_M and the structure of the PEV depend on network features. Given the adjacency matrix, the determination of the largest eigenpair is numerically not difficult, by means of the straightforward power-iteration method [13], even for the largest structures. However, understanding what determines the largest eigenpair is a very important task, since it allows us to efficiently control and manipulate spectral properties and the associated dynamical effects [27,20,31].

A first, seminal result in this endeavor was provided by Chung, Lu and Vu [8] (CLV), who derived, for a class of maximally random networks with given expected degree distribution, a formula relating the LEV with simple topological properties of the network, namely the first moments of the degree distribution and the overall largest degree, $q_{\max}$. In the limit of networks of infinite size the CLV expression can be recast as [3]

$$\Lambda_M \approx \max\{\sqrt{q_{\max}}, \langle q^2\rangle/\langle q\rangle\}, \tag{1}$$

which turns out to be remarkably accurate for random uncorrelated networks of any size [5], as generated with the uncorrelated configuration model (UCM) [6]. Eq. (1) can be physically interpreted as follows [4]: the largest eigenvalue of the whole structure is given by the largest among the eigenvalues of two network subgraphs, considered as isolated. The first of these subgraphs is the star graph formed by the node with largest degree (the hub) and its nearest neighbors, with a LEV $\Lambda_M^{(star)} = \sqrt{q_{\max}}$ [30]. The second is the densely interconnected subgraph identified, in the K-core decomposition procedure [29], as the K-core with maximum index K_M. This subgraph, being homogeneous, has a LEV well approximated by its internal average degree, $\Lambda_M^{(K_M)} \approx \langle q\rangle_{K_M}$. In Ref. [9] it is shown that the internal average degree of the maximum K-core can be approximated by the excess average degree of the whole network, $\langle q^2\rangle/\langle q\rangle$. Therefore, we have $\Lambda_M^{(K_M)} \approx \langle q^2\rangle/\langle q\rangle$. This interpretation is validated by the observation that, in random uncorrelated networks, when the global LEV is given by $\sqrt{q_{\max}}$, the PEV is localized on the star graph composed by the hub and its neighbors; in the other case the PEV is instead localized on the max K-core [22] .

While Eq. (1) predicts very well the LEV for random uncorrelated networks, it often fails when applied to real-world networks [5]. Recently, the original CLV formula has been modified to extend its validity beyond the uncorrelated case [5]:

$$\Lambda_M \approx \max\{\sqrt{q_{\max}}, \langle q\rangle_{K_M}\}, \tag{2}$$

where $\langle q\rangle_{K_M}$ is the average degree of the max K-core subgraph. The physics behind Eq. (2) is the same as in the uncorrelated case: the value of the LEV is determined by the competition among two subgraphs, the star centered around the hub and the max K-core. What changes with respect to the uncorrelated case is the expression of $\Lambda_M^{(K_M)}$, which may largely differ from the ratio between the second and the first moment of the degree distribution. Eq. (2) has been empirically tested on a large set of real-world networks, for which a good accuracy in the prediction of the actual value of Λ_M was observed [5].

In this paper we push further the analysis of Ref. [5], by studying in detail the localization properties of the PEV in real networks, spelling out some of its implications and checking their validity in real-world networks. After reviewing established results for synthetic networks, we analyze a set of 38 real-world topologies of diverse origin, with the goal of determining whether the dominating term in Eq. (2) allows us to infer where the PEV is localized. While

this picture is most of the time correct, we uncover the existence of some exceptions: networks with the PEV localized on both subgraphs and (more surprisingly) networks with the PEV localized on a set of nodes with no overlap with the star surrounding the hub or the max K-core. In addition, we investigate how the PEV localization nontrivially affects a dynamical (epidemic) process mediated by the network topology. The removal of the hub or of the max K-core can lead to negligible effects or to a complete disruption of the epidemic dynamics, depending on the PEV localization properties.

2 Localization on subgraphs in synthetic networks

We first consider the localization of the PEV on synthetic uncorrelated networks with a power-law degree distribution of the form $P(q) \sim q^{-\gamma}$, generated using the uncorrelated configuration model (UCM) [6]. For the PEV $\{f_i\}$, normalized as $\sum_i f_i^2 = 1$, the localization in ensembles of synthetic networks of varying size can be assessed by studying the inverse participation ratio (IPR) Y_4, defined as

$$Y_4(N) = \sum_i f_i^4, \tag{3}$$

as a function of the network size N [12,19]. Different types of localization reflect in the functional form of the IPR as a function of N, expressed as a power-law [22]:

$$Y_4(N) \sim N^{-\alpha}. \tag{4}$$

If the PEV is delocalized, i.e., homogeneously distributed over all nodes in the network, then $f_i \simeq N^{-1/2}$, $\forall i$. In this case $Y_4(N) \sim N^{-1}$ and $\alpha = 1$. If the PEV is instead homogeneously localized on a set of nodes V of size N_v, then $f_i \simeq N_V^{-1/2}$ for $i \in V$, and $f_i \simeq 0$ for $i \notin V$. In this case, we have $Y_4(N) \sim N_V^{-1}$. If V is a subextensive set of nodes, with size N_V growing with the size N of the whole network as $N_V \sim N^{\delta}$, then $\alpha = \delta$. In the extreme case of localization of a set of nodes with fixed size, $N_V = \text{const.}$ (including the case of a single node), then $\alpha = 0$. Other more complex forms of localization are possible as well. One that plays a relevant role in this work is the one occurring on a star graph formed by a hub connected to $q_{\max}$ nodes (leaves). In such a case, it is easy to see, applying Perron-Frobenius theorem [11], that the LEV is $\Lambda_M = \sqrt{q_{\max}}$, and that the hub has weight $f_{hub} = 1/\sqrt{2}$, while each of the leaves carries a weight $f_i = 1/\sqrt{2q_{\max}}$. As a consequence the total weight is equally split among the hub and the set of all leaves. In this case, $Y_4(q_{\max}) = \frac{1}{4}(1 - q_{\max}^{-1})$, and the IPR goes asymptotically to $1/4$ as $q_{\max}$ diverges.

In Fig. 1a) we first check the validity of the original CLV result, Eq. (1), by plotting the largest eigenvalue Λ_M as a function of $\max\{\sqrt{q_{\max}}, \langle q^2\rangle/\langle q\rangle\}$. In order to avoid complications, we consider only networks with a single node with maximum degree $q_{\max}$. As we can observe, Eq. (1) fits the empirical data with an excellent precision. Given the form of Eq. (1), for a power-law degree distribution $P(q) \sim q^{-\gamma}$ with $\gamma \leq 5/2$ the LEV is given by $\langle q^2\rangle/\langle q\rangle$, and the PEV is expected to be localized on the max K-core. For $\gamma > 5/2$, on the other hand, the LEV takes the form $\sqrt{q_{\max}}$, and the PEV is localized on the hub. In Fig. 1b) we check this conjecture by plotting the IPR as a function of N. In accordance with our expectation, for large γ the value of $Y_4(N)$ tends to a constant for large N, which is compatible with localization on the hub and its neighbors, while for small γ, it decreases with N. The decrease for $\gamma \leq 5/2$ is however slower than N^{-1}, indicating the absence of complete delocalization [22]. The PEV is in this case localized on a subextensive set, which

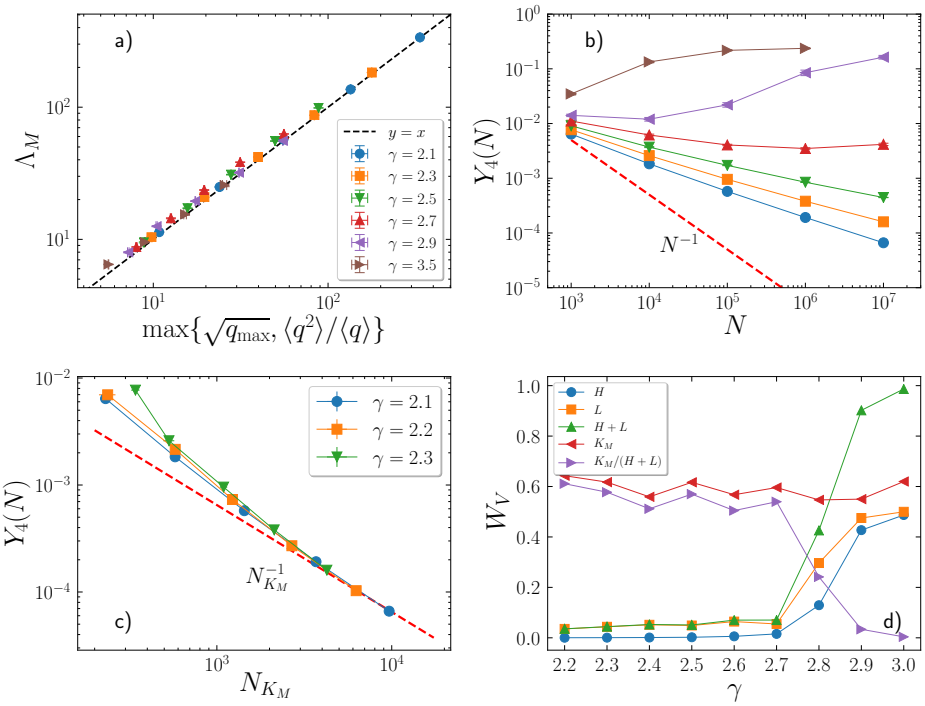


Fig. 1 Spectral properties of uncorrelated UCM networks. (a) Largest eigenvalue Λ_M as a function of the theoretical prediction Eq. (1) for networks sizes from $N = 10^3$ to 10^7 (b) Inverse participation ratio Y_4 as a function of network size. (c) Inverse participation ratio as a function of the size of the max K-core N_{K_M}. (d) Relative weight W_V of different network subgraphs V (see main text). Network size is in this case $N = 10^7$.

is identified as the max K-core in Fig. 1c), where we plot $Y_4(N)$ as a function of the max K-core size, and observe a trend $Y_4 \sim N_{K_M}^{-1}$ for large N.

A correct characterization of the PEV localization in UCM networks is somewhat impeded by the fact that the hub and some of its neighbors usually belong to the max K-core. In order to properly discriminate the weight contribution of each one of the relevant subgraphs, in Fig. 1d) we plot the relative weight

$$W_V = \sum_{i \in V} f_i^2 \tag{5}$$

for different sets of nodes: the hub alone, $V = H$; the set of hub neighbors (leaves), $V = L$; the star defined by the hub and the leaves, $V = H + L$; the complete max K-core, $V = K_M$; and the max K-core, excluding hubs and leaves, $V = K_M \setminus (H + L)$. As we can observe, for small γ the weight is dominated by the max K-core, with a very small contribution from the leaves and the hub inside it. For large γ, on the other hand, the contribution of the hub and the leaves increases, in such a way as to almost dominate the whole PEV weight for the largest γ considered. In this regime, however, the max K-core still represents a sizeable fraction of the total weight. This is due to the fact that, even though in the limit $\gamma \to 3$ the max K-core diminishes in size [9], it always contains the hub and a fraction of the leaves, which are the responsible for its large weight. When subtracting the weight of the hub and of the leaves it contains, the remaining max K-core shows a vanishing weight. These observations

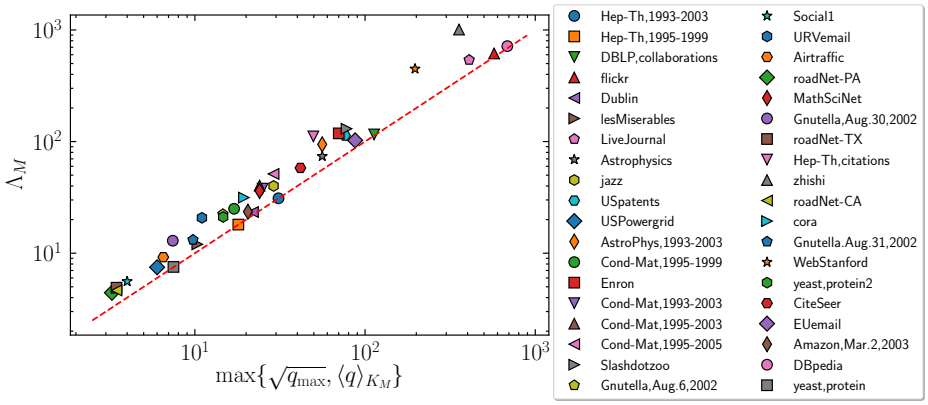


Fig. 2 Largest eigenvalue Λ_M as a function of the theoretical prediction Eq. (2) for the 38 networks real networks listed in Table 1.

indicate that, for large γ, we are in the presence of a localization on the star surrounding the hub. The weight is equally divided between the hub and the $q_{\max}$ leaves, i.e., $f_i^2 \sim 1/2$, $i \in H$, and $f_i^2 \sim 1/(2q_{\max})$, $i \in L$. The rest of the network has a vanishing weight. In this case, $Y_4(N) \sim (1/2)^2 + (1/2)^2/q_{\max}$, which still goes to a constant for sufficiently large N, in agreement with the result in Fig. 1b).

3 Localization on subgraphs in real networks

In analogy with the case of uncorrelated networks, it is very natural to conjecture, from Eq. (2), that when Λ_M practically coincides with $\Lambda_M^{(star)}$ then the PEV is localized on the hub and its immediate neighbors; vice versa, when $\Lambda_M \approx \Lambda_M^{(K_M)}$ the PEV is localized on the max K-core. To test this hypothesis we consider a subset of the real networks analyzed in Ref. [5] given by those networks in which the hub does not belong to the max K-core. We do not consider networks in which the hub belongs to the max K-core since in that case it is difficult to discriminate between a PEV localized only on the hub and its neighbors or on all the max K-core. This criterion leaves us with 38 topologies, listed in Table 1 (see Appendix). The validity of Eq. (2) for those networks is illustrated in Fig. 2.

In the case of real networks, for which only a single snapshot of a fixed size is available, the direct inspection of the IPR does not provide enough information, since a size dependence cannot be estimated as for synthetic networks. In this case, therefore, we consider the relative weights W_{K_M} and W_{Star} on the max K-core and on the star formed by the hub and its leaves, respectively, which give a measure of the total weight concentrated on each of these subgraphs. In Fig. 3 we present a scatter plot of these two relative weights. The labels refer to the network numbers presented in Table 1. It turns out that most networks are actually strongly localized either on the max K-core (large W_{K_M}, very small W_{Star}) or around the hub (large W_{Star}, very small W_{K_M}). However, the picture is more complicated than what could be naively anticipated, and several exceptions are evident. The color code of each point provides additional information, representing the ratio d_{star}/d_{K_M} between the relative distances of

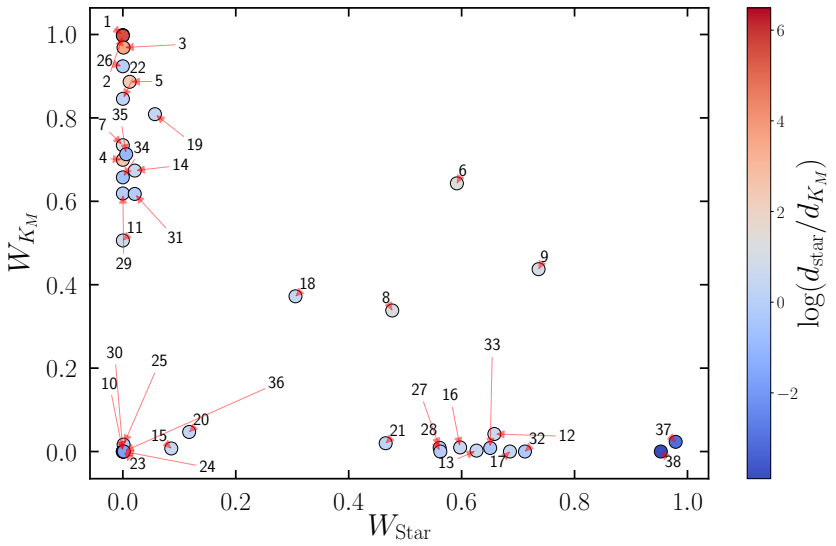


Fig. 3 Scatter plot of the total PEV weight localized on the max K-core (W_{K_M}) versus the total PEV weight localized on the star graph around the hub (W_{Star}) in the real networks considered. Points are identified by the network order in Table 1. The color of the symbols encodes the ratio d_{star}/d_{K_M}, see Table 1.

subgraphs largest eigenvalues to the global Λ_M:

$$d_{star} = \frac{\Lambda_M - \Lambda_M^{(star)}}{\Lambda_M}, \tag{6}$$

$$d_{K_M} = \frac{\Lambda_M - \Lambda_M^{(K_M)}}{\Lambda_M}. \tag{7}$$

If the ratio d_{star}/d_{K_M} is much larger or much smaller than 1, then the naive expectation is correct: the PEV is strongly localized on the subgraph with largest eigenvalue. However, if the ratio is not very different from 1 (i.e., in a range approximately between 0.4 and 2) the naive expectation is not predictive: in some cases $\Lambda_M^{(K_M)} > \Lambda_M^{(star)}$, yet the PEV is localized on the star; the opposite case also occurs. This result can be understood by considering that the localization can occur on a densely interconnected network subset, for which the max K-core is only an approximation. Moreover, $\langle q \rangle_{K_M}$ is in its turn only an approximation of largest eigenvalue of the max K-core. This is why Eq. (2) is an approximate formula for Λ_M and, if the two quantities appearing on the r.h.s. are not too different, one cannot strictly deduce where the PEV is localized from which of the two quantities is largest.

Further support to this interpretation is provided by Fig. 4, in which we report, for each real network, the fraction of the total weight W_V localized on the hub (H), on the intersection of the max K-core and the leaves ($K_M \cap L$), on the leaves not belonging to the max K-core ($L \setminus K_M$), and on nodes belonging in the max K-core that are not leaves ($K_M \setminus L$). In the four networks having large PEV weight on both subsets, there is a considerable weight localized on nodes shared by the two subsets; in other words, some neighbors of the hub are also part of the max K-core: the subsets have a strong overlap and this explains why both W_{K_M} and W_{H+L} are large.

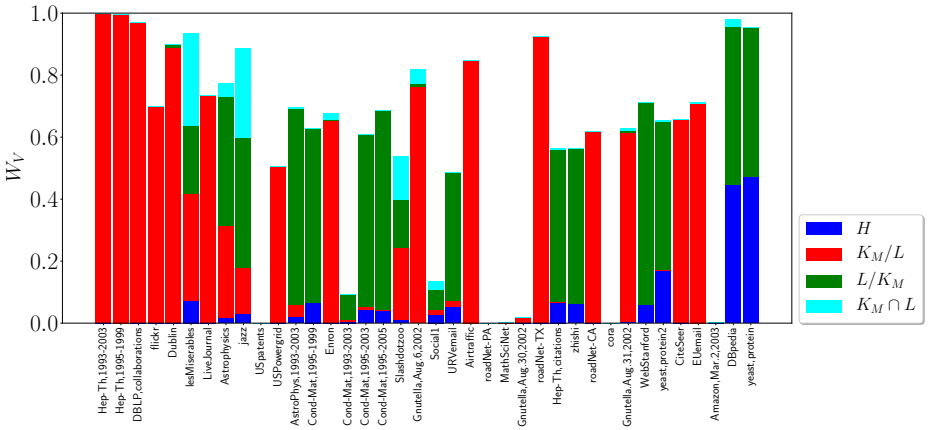


Fig. 4 For each of the real networks considered, we plot the total PEV weight concentrated on the hub, W_H; on the intersection of the max K-core and of the hub leaves, $W_{K_M \cap L}$; on the leaves not belonging to the max K-core, $W_{L \setminus K_M}$; and on the nodes in the max K-core that are not leaves, $W_{K_M \setminus L}$.

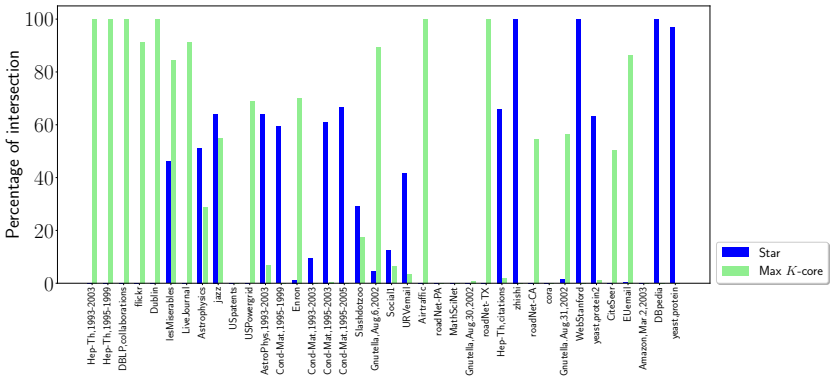


Fig. 5 Intersection of the empirical localization set obtained from a greedy algorithm with the star and the max K-core subgraphs of the real networks considered.

Finally, a handful of networks in Fig. 3 have vanishing small weight on both subsets considered. This is a priori not surprising: the PEV could be fully delocalized. However, it turns out that these networks are actually localized, but on sets different from the star or the max K-core; nevertheless the value of the LEV is still approximately described by Eq. (2).

This same picture can be recovered if one estimates the empirical localization set $\mathscr{L}$ of each real network by applying a greedy algorithm. In this approach, the PEV components f_i^2 are ordered in decreasing value, and the localization set is defined by the smallest number of nodes carrying a weight larger than or equal to a given threshold W_c. In Fig. 5 we show the intersection of the empirical localization set $\mathscr{L}$ obtained for a threshold $W_c = 0.75$ with both the star and the max K-core subgraphs. This figure recovers essentially the features observed in Fig. 4: a majority of networks have an empirical localization set that coincides essentially with the star or the max K-core subgraphs, in accordance, with some exceptions with the LEV criteria (networks in the Fig. 5 are ordered in decreasing ratio d_{star}/d_{K_M}, see

Table 1). Some other networks, in particular `USPatents` (10), `roadNet-PA` (23), `MathSciNet` (24), and `cora` (30), are localized in sets with almost null overlap with both the star and the max K-core. Accordingly, these networks fall in the bottom left corner of Fig. 3.

4 Consequences for epidemic dynamics

The PEV localization on different network subgraphs is an important piece of information that can be exploited to modify and control dynamical processes mediated by the network topology. An immediate example is provided by the susceptible-infected-susceptible (SIS) model for epidemic spreading on networks [23]. According to this model, individuals sit on the nodes of a network (representing the contact pattern among them). Each individual can be either healthy but susceptible (S) to contract the disease or infected (I) and able to transmit the infection to his/her contacts. For each contact between an individual in state I and one in state S there is a rate of transmission β, while each infected agent can spontaneously recover at rate μ. The ratio $\lambda = \beta/\mu$ is the control parameter of the model, determining whether in the stationary state all individuals are in state S (for $\lambda \leq \lambda_c$) or a finite fraction of them is infected (for $\lambda > \lambda_c$). The quenched mean-field approach to these dynamics [33,32,3] predicts that the epidemic threshold is the inverse of the adjacency matrix's LEV, $\lambda_c = 1/\Lambda_M$. We note here that the SIS dynamics is ruled by the spectral properties of the adjacency matrix because reinfection events between connected nodes play a fundamental role in sustaining the steady state characterizing the model [4]. In other epidemic processes without a steady state, such as the SIR model, reinfection events ("backtracking paths") are not allowed, and thus the dynamical properties in this case are described by the spectral properties of the non-backtracking matrix [18,14,15].

One of the crucial problems in epidemic spreading is preventive immunization [34]: if it is possible to vaccinate only some individuals, how should they be selected in order to minimize the probability of an epidemic to occur and its extension? Different strategies have been proposed. Among them a naturally appealing one is degree-based selection: nodes with higher degree should be vaccinated first [24]. The results presented in the previous section suggest that the effect of immunizing high-degree individuals can be completely different depending on where the PEV is localized. To show this, let us consider two networks with completely different properties concerning PEV localization: `DBpedia` (strongly localized on the star graph around the hub) and `Hep-Th,1995-1999` (strongly localized on the max K-core). In these networks, we immunize only the node with largest degree, effectively removing it from the network. A first measure of the different effects of this immunization for the two networks is the relative reduction of the LEV Λ_M. The original networks have a LEV (see Table 1) $\Lambda_M = 716.3$ for `DBpedia` and $\Lambda_M = 18.04$ for `Hep-Th,1995-1999`. The resulting networks after the removal of the hub have instead LEVs $\Lambda'_M = 563.6$ for `DBpedia` and $\Lambda'_M = 18.04$ for `Hep-Th,1995-1999`. Therefore, while the removal of the hub does not affect the LEV of `Hep-Th,1995-1999`, it induces a 21% decrease in `DBpedia`.

The different effect of the removal of a single individual on the epidemic spreading is most clearly seen in Fig. 6, where we plot the order parameter $\langle\rho\rangle$, defined as the average number of infected individuals in the steady state, and the susceptibility χ, defined as

$$\chi = N\frac{\langle\rho^2\rangle - \langle\rho\rangle^2}{\langle\rho\rangle}, \tag{8}$$

evaluated around the epidemic transition both in the presence and in the absence of the hub. Results are obtained by applying the quasi-stationary simulation method [10].

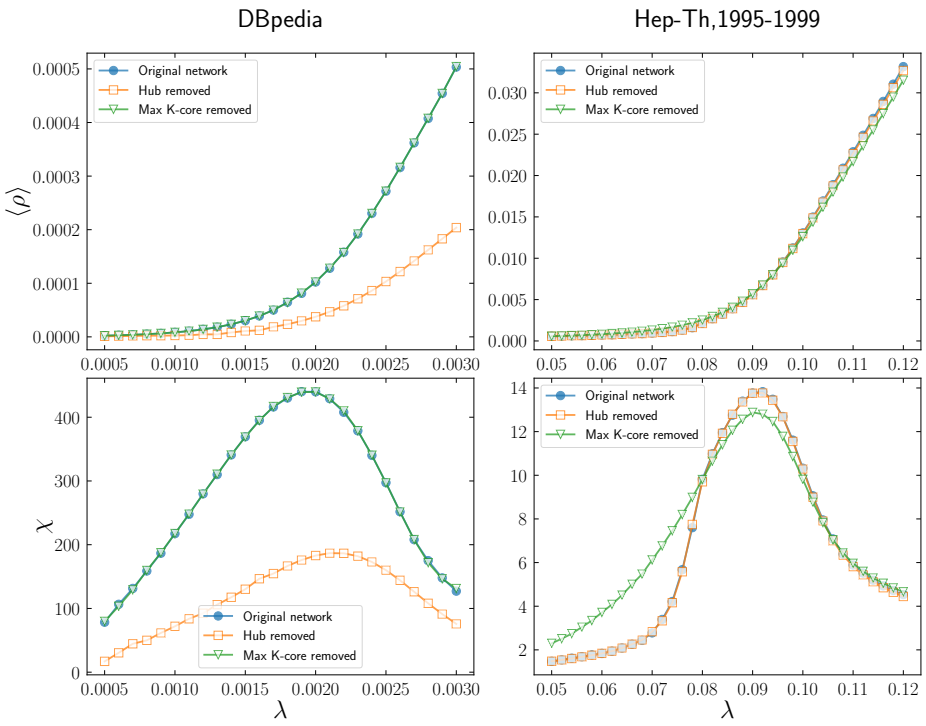


Fig. 6 Results of simulations of the SIS model on the `DBpedia` (left column) and `Hep-Th,1995-1999` (right column) networks. Top plots: density $\langle\rho\rangle$ of nodes in the infected state in the quasi-stationary state. Bottom plots: susceptibility $\chi = N(\langle\rho^2\rangle - \langle\rho\rangle^2)/\langle\rho\rangle$.

The removal of the hub has virtually no effect in the case of `Hep-Th,1995-1999`, where the localization occurs on the max K-core. This is expected based on the physical picture underlying Eq. (2): even if the hub is immunized, the dense web of contacts among the other nodes in the max K-core is as effective as before in triggering the epidemic transition. A completely different scenario emerges when the localization occurs around the hub, as in `DBpedia`. The vaccination of the center of the star graph completely destroys the local structure triggering the epidemics, leading to a very strong reduction in the extent of the infection. Notice that this is the effect of the removal of just one individual out of more than 3 million. With respect to the number of edges removed, in the case of `DBpedia` immunization of the hub amounts to the removal of 3.7% of edges, while in `Hep-Th,1995-1999` it implies the deletion of less than 0.4% of edges. Such difference in the fraction of edges removed cannot does not account for the strong effect observed.

In the same Fig. 6, we present also the results obtained for SIS dynamics on the two networks considered, when the nodes belonging to the maximum K-core have been immunized. In the case of `DBpedia`, the immunization of the max K-core produces essentially no effect at all, in agreement with the picture in which the weight of the PEV is strongly localized in the hub and its neighbors. On the other hand, the max K-core immunization in the `Hep-Th,1995-1999` network induces a noticeable variation in the SIS dynamics, with a stronger effect at the level of the susceptibility χ. This is again in agreement with the fact the that PEV is, in this case, localized on the max K-core. While the effect is in appearance

small, one must bear in mind that it is produced by the immunization of a max K-core of size 19, implying the removal of barely 1.3% of edges, which is sufficient to induce a variation of a 20.4% in the value of the LEV.

The two examples presented are the most extreme. For other networks, with weaker localization on subgraphs, one expects less strong, yet similar, effects.

5 Conclusions

The principal eigenvector (PEV) of the adjacency matrix characterizing complex networks has interesting localization properties, which are associated with the spread and containment of diseases in networked substrates. In this work, leveraging the results of Ref. [5], we have shown that the localization of the PEV in real empirical networks is often strongly correlated with the value of its associated largest eigenvalue (LEV), and in its turn, with the network subgraph that dominates this LEV. In this sense, the LEV is essentially given by the maximum between the largest eigenvalue of two well-defined subgraphs: the star formed by node of largest degree (hub) and its nearest neighbors, and the densely connected subgraph given by the maximum core in a K-core decomposition. When the global LEV is very close to the LEV of one of these subgraphs, the PEV is correspondingly strongly localized in that subgraph. This picture applies in general, but with non negligible exceptions. The predictive power of our result depends on how close the LEV is to one of the subgraph LEV's, and thus on the distance between these subgraph LEV's. When the LEV of the whole network is very close to the LEV of a sugbraph, strong localization ensues. When the LEV is at an intermediate position, different levels of localization mixing between the subgraphs are possible. In other cases, moreover, localization can be strong, but in a subgraph with no intersection with either the star or the max K-core, depending on particular features of the network's topology.

Our results have a bearing also on the behavior of epidemic processes on networks. Indeed, the subgraph in which the PEV is localized has been identified with the activation set of epidemic spreading [4]. Here we show that the fact that the localization subgraph can be a K-core, independent of the hub, renders usual degree-based immunization strategies useless, since the vaccination of the hub can leave almost untouched the K-core, where epidemic activation is centered. Our results open thus the path for the research of more global immunization strategies, taking into account the full spectral structure of complex networks.

References

1. Barrat, A., Barthélemy, M., Vespignani, A.: Dynamical Processes on Complex Networks. Cambridge University Press, Cambridge (2008)
2. Brin, S., Page, L.: The anatomy of a large scale hypertextual Web search engine. Comput. Networks ISDN Syst. **30**(1/7), 107–17 (1998). DOI 10.1.1.109.4049
3. Castellano, C., Pastor-Satorras, R.: Thresholds for epidemic spreading in networks. Phys. Rev. Lett. **105**, 218,701 (2010). DOI 10.1103/PhysRevLett.105.218701
4. Castellano, C., Pastor-Satorras, R.: Competing activation mechanisms in epidemics on networks. Scientific Reports **2**, 00,371 (2012)
5. Castellano, C., Pastor-Satorras, R.: Relating topological determinants of complex networks to their spectral properties: Structural and dynamical effects. Phys. Rev. X **7**, 041,024 (2017). DOI 10.1103/PhysRevX.7.041024
6. Catanzaro, M., Boguñá, M., Pastor-Satorras, R.: Generation of uncorrelated random scale-free networks. Phys. Rev. E **71**, 027,103 (2005)
7. Chakrabarti, D., Wang, Y., Wang, C., Leskovec, J., Faloutsos, C.: Epidemic thresholds in real networks. ACM Trans. Inform. Syst. Sec. **10**, 13 (2008)

8. Chung, F., Lu, L., Vu, V.: Spectra of random graphs with given expected degrees. Proc. Natl. Acad. Sci. USA **100**, 6313–6318 (2003)
9. Dorogovtsev, S.N., Goltsev, A.V., Mendes, J.F.F.: k-core organization of complex networks. Phys. Rev. Lett. **96**(4), 040,601 (2006). DOI 10.1103/PhysRevLett.96.040601
10. Ferreira, S.C., Castellano, C., Pastor-Satorras, R.: Epidemic thresholds of the susceptible-infected-susceptible model on networks: A comparison of numerical and theoretical results. Phys. Rev. E **86**, 041,125 (2012)
11. Gantmacher, F.R.: The theory of matrices, vol. II. Chelsea Publishing Company, New York (1974)
12. Goltsev, A.V., Dorogovtsev, S.N., Oliveira, J.G., Mendes, J.F.F.: Localization and spreading of diseases in complex networks. Phys. Rev. Lett. **109**, 128,702 (2012). DOI 10.1103/PhysRevLett.109.128702
13. Golub, G.H., Van Loan, C.F.: Matrix computations, vol. 3. JHU Press, Baltimore (2012)
14. Karrer, B., Newman, M.E.J.: Message passing approach for general epidemic models. Physical Review E **82**(1), 016,101 (2010). DOI 10.1103/PhysRevE.82.016101. URL `http://link.aps.org/doi/10.1103/PhysRevE.82.016101`
15. Karrer, B., Newman, M.E.J., Zdeborová, L.: Percolation on sparse networks. Phys. Rev. Lett. **113**, 208,702 (2014). DOI 10.1103/PhysRevLett.113.208702
16. Katz, L.: A new status index derived from sociometric analysis. Psychometrika **18**(1), 39–43 (1953). DOI 10.1007/BF02289026
17. Kinouchi, O., Copelli, M.: Optimal dynamical range of excitable networks at criticality. Nat Phys **2**(5), 348–351 (2006)
18. Krzakala, F., Moore, C.: Spectral redemption in clustering sparse networks. Proceedings of the National Academy of Sciences **110**(52), 20,935–40 (2013). DOI 10.1073/pnas.1312486110. URL `http://www.pubmedcentral.nih.gov/articlerender.fcgi?artid=3876200{&}tool=pmcentrez{&}rendertype=abstract{%}5Cnhttp://www.pnas.org/content/110/52/20935.short`
19. Martin, T., Zhang, X., Newman, M.E.J.: Localization and centrality in networks. Phys. Rev. E **90**, 052,808 (2014)
20. Milanese, A., Sun, J., Nishikawa, T.: Approximating spectral impact of structural perturbations in large networks. Phys. Rev. E **81**, 046,112 (2010). DOI 10.1103/PhysRevE.81.046112. URL `https://link.aps.org/doi/10.1103/PhysRevE.81.046112`
21. Newman, M.: Networks: An Introduction. Oxford University Press, Inc., New York, NY, USA (2010)
22. Pastor-Satorras, R., Castellano, C.: Distinct types of eigenvector localization in networks. Sci. Rep. **6**, 18,847 (2016). DOI 10.1038/srep18847
23. Pastor-Satorras, R., Castellano, C., Van Mieghem, P., Vespignani, A.: Epidemic processes in complex networks. Rev. Mod. Phys. **87**, 925–979 (2015)
24. Pastor-Satorras, R., Vespignani, A.: Immunization of complex networks. Phys. Rev. E **65**(3), 036,104 (2002). DOI 10.1103/PhysRevE.65.036104
25. Pomerance, A., Ott, E., Girvan, M., Losert, W.: The effect of network topology on the stability of discrete state models of genetic control. Proceedings of the National Academy of Sciences **106**(20), 8209–8214 (2009). DOI 10.1073/pnas.0900142106
26. Restrepo, J.G., Ott, E., Hunt, B.R.: Onset of synchronization in large networks of coupled oscillators. Phys. Rev. E **71**, 036,151 (2005). DOI 10.1103/PhysRevE.71.036151
27. Restrepo, J.G., Ott, E., Hunt, B.R.: Characterizing the dynamical importance of network nodes and links. Phys. Rev. Lett. **97**, 094,102 (2006). DOI 10.1103/PhysRevLett.97.094102. URL `https://link.aps.org/doi/10.1103/PhysRevLett.97.094102`
28. Restrepo, J.G., Ott, E., Hunt, B.R.: Weighted percolation on directed networks. Phys. Rev. Lett. **100**, 058,701 (2008). DOI 10.1103/PhysRevLett.100.058701
29. Seidman, S.B.: Network structure and minimum degree. Social Networks **5**, 269 –287 (1983). DOI DOI:10.1016/0378-8733(83)90028-X
30. Van Mieghem, P.: Graph Spectra for Complex Networks. Cambridge University Press, Cambridge, U.K. (2011)
31. Van Mieghem, P., Stevanović, D., Kuipers, F., Li, C., van de Bovenkamp, R., Liu, D., Wang, H.: Decreasing the spectral radius of a graph by link removals. Phys. Rev. E **84**, 016,101 (2011). DOI 10.1103/PhysRevE.84.016101. URL `https://link.aps.org/doi/10.1103/PhysRevE.84.016101`
32. Van Mieghem, P., Omic, J., Kooij, R.E.: Virus spread in networks. IEEE/ACM Transactions on Networking **17**(1), 1–14 (2009)
33. Wang, Y., Chakrabarti, D., Wang, C., Faloutsos, C.: Epidemic spreading in real networks: An eigenvalue viewpoint. In: 22nd International Symposium on Reliable Distributed Systems (SRDS'03), pp. 25–34. IEEE Computer Society, Los Alamitos, CA, USA (2003)
34. Wang, Z., Bauch, C.T., Bhattacharyya, S., d'Onofrio, A., Manfredi, P., Perc, M., Perra, N., Salathé, M., Zhao, D.: Statistical physics of vaccination. Physics Reports **664**(Supplement C), 1 – 113 (2016). DOI https://doi.org/10.1016/j.physrep.2016.10.006. URL `http://www.sciencedirect.com/science/article/pii/S0370157316303349`. Statistical physics of vaccination

Appendix

In this appendix we present data about the real-world networks considered in the analysis.

	Network	$d_{\rm star}/d_{\rm K_M}$	N	$W_{\rm H+L}$	$W_{\rm K_M}$	Λ_N	$\sqrt{q_{\rm max}}$	$\langle q\rangle_{\rm K_M}$	$N_{\rm K_M}$
1	Hep-Th,1993-2003	659.3	8638	3.9e-05	0.9987	31.03	8.062	31	32
2	Hep-Th,1995-1999	248.2	5835	7.129e-10	0.9971	18.04	7.071	18	19
3	DBLP,collaborations	34.19	317080	0.001186	0.9686	115.8	18.52	113	114
4	flickr	12.73	105722	5.479e-05	0.6996	615.6	73.65	573	574
5	Dublin	11.29	410	0.01207	0.8866	23.38	7.071	21.94	32
6	lesMiserables	3.591	77	0.5916	0.643	12.01	6	10.33	12
7	LiveJournal	3.201	5189808	1.123e-07	0.7345	539	122.5	408.9	415
8	Astrophysics	3.07	14845	0.4771	0.3382	73.89	18.97	56	57
9	jazz	2.723	198	0.7363	0.4372	40.03	10	29	30
10	USpatents	2.309	3764117	8.901e-06	2.185e-11	113	28.16	76.28	106
11	USPowergrid	2.107	4941	1.013e-20	0.506	7.483	4.359	6	12
12	AstroPhys,1993-2003	1.873	17903	0.658	0.04205	94.43	22.45	56	57
13	Cond-Mat,1995-1999	1.834	13861	0.6264	0.002197	24.98	10.34	17	18
14	Enron	1.68	33696	0.02111	0.6737	118.4	37.19	70.06	275
15	Cond-Mat,1993-2003	1.644	21363	0.08579	0.007321	37.89	16.7	25	26
16	Cond-Mat,1995-2003	1.6	27519	0.5974	0.009829	40.31	14.21	24	25
17	Cond-Mat,1995-2005	1.553	36458	0.6856	3.991e-10	51.29	16.67	29	30
18	Slashdotzoo	1.522	79116	0.3057	0.3721	130.4	50.34	77.8	129
19	Gnutella,Aug.6,2002	1.499	8717	0.05683	0.8089	22.38	10.72	14.61	175
20	Social1	1.43	67	0.1174	0.04684	5.591	3.317	4	5
21	URVemail	1.264	1133	0.4655	0.01989	20.75	8.426	11	12
22	Airtraffic	1.258	1226	0.0001306	0.8458	9.209	5.831	6.523	107
23	roadNet-PA	1.219	1087562	2.651e-38	1.89e-14	4.42	3	3.255	916
24	MathSciNet	1.143	332689	0.001357	2.804e-07	36.09	22.27	24	25
25	Gnutella,Aug.30,2002	0.9298	36646	0.001329	0.01666	12.93	7.416	7	14
26	roadNet-TX	0.9287	1351137	9.823e-48	0.9238	4.906	3.464	3.353	1491
27	Hep-Th,citations	0.9166	27400	0.5611	0.008903	111.3	49.68	44.08	52
28	zhishi	0.8983	372840	0.5623	1.182e-11	1008	356.5	282.7	449
29	roadNet-CA	0.8905	1957027	1.499e-09	0.6189	4.638	3.464	3.32	4454
30	cora	0.8594	23166	4.556e-05	4.623e-06	31.5	19.42	17.44	25
31	Gnutella.Aug.31,2002	0.8357	62561	0.0211	0.6177	13.18	9.747	9.072	1004
32	WebStanford	0.749	255265	0.7121	2.445e-05	448.1	196.5	112.2	387
33	yeast,protein2	0.6756	2172	0.6506	0.008435	21.1	14.66	11.57	14
34	CiteSeer	0.5007	365154	2.891e-05	0.6574	58.08	41.7	25.37	1850
35	EUemail	0.3844	224832	0.005901	0.7129	102.5	87.38	63.12	292
36	Amazon,Mar.2,2003	0.1807	262111	0.001668	3.41e-05	23.55	20.49	6.643	286
37	DBpedia	0.04497	3915921	0.9791	0.02326	716.3	685.3	27.89	70
38	yeast,protein	0.02039	1458	0.9528	4.17e-06	7.535	7.483	5	6

Table 1 Topological and spectral properties of the real networks considered: Ratio of the distance between the actual largest eigenvalue Λ_M and the LEV's of the relevant subgraphs (star centered at the hub and max K-core), $d_{\rm star}/d_{\rm K_M}$; network size N, relative weight of the PEV on the star centered in the hub, $W_{\rm H+L}$; relative weight of the PEV on the max K-core, $W_{\rm K_M}$; largest eigenvalue Λ_M; square root of the maximum degree, $\sqrt{q_{\rm max}}$; average degree of the max K-core, $\langle q\rangle_{\rm K_M}$; size of the max K-core, $N_{\rm K_M}$.